Atomistic simulation studies of iron sulphide, platinum antimonide and platinum arsenide

P.E. Ngoepe[a,b*], P.S. Ntoahae[a], S.S. Mangwejane[a], H.M. Sithole[c], S.C. Parker[d], K.V. Wright[e] and N.H. de Leeuw[f]

We present the results of atomistic simulations using derived interatomic potentials for the pyrite-structured metal chalcogenides FeS_2, $PtSb_2$ and $PtAs_2$. Structural and elastic constants were calculated and compared with experimental measurements. Surface energies of low-index surfaces were calculated and closely reflected the measured stabilities of these compounds. Equivalent surfaces on the pyrite and marcasite structures of FeS_2 explained the experimentally observed intergrowths of the two phases.

Introduction

Metal sulphide minerals are of industrial significance because they serve as a source of various metals. Pyrite (FeS_2) is the most common of these minerals and is found in both igneous and sedimentary rocks. In addition, it is a major phase in massive sulphur ore deposits of base, ferroalloy and precious metals. The platinum group minerals consist mainly of platinum group element (PGE) compounds including sulphides, arsenides and antimonides, and are attached to or enclosed by base metal sulphides, silicate and chromite grains.[1] An understanding of the bulk and surface properties of these compounds is necessary for the recovery of minerals from ore deposits, such as in mineral separation techniques. Detailed knowledge of the reactivity of the surfaces with water and surfactants used for extraction is important in the design of an efficient flotation scheme.

Numerous experimental studies[2–4] have been carried out on the structural, electronic and optical properties of pyrite and quantum mechanical *ab initio* calculations[5–7] performed. FeS_2 crystallizes in an orthorhombic marcasite as well as in a cubic pyrite structure. Possible intergrowths have been reported between these phases, along the {100} and {101} surfaces of pyrite and marcasite, respectively.[8] The pyrite structure is also adopted by some of the platinum group minerals, such as $PtSb_2$[9] and $PtAs_2$,[10] which also serve as sources of platinum. Although studies on these compounds are limited compared to those on FeS_2, experimental information is available on the semiconducting and elastic properties of $PtSb_2$.[11]

Atomistic simulations using interatomic potentials have matured to the point where they can benefit studies of materials. Their combination with experimental methods has produced insights into bulk, surface and transport properties, particularly of metal oxides,[12] which are mainly ionic. The current work is part of a continuing effort to derive and validate robust interatomic potentials in metal sulphides,[13,14] as a basis for atomistic simulation studies of base and precious metal sulphides, whose atoms are predominantly covalently bonded. Our ultimate intention is to be able to model systems with a large number of atoms (from tens to a hundred thousand) with minimal computational resources. This approach should facilitate simulation studies of surfaces, crystal growth and mineral separation.

[a]Materials Modelling Centre, University of Limpopo, Sovenga 0727, South Africa.
[b]Manufacturing and Materials Technology, CSIR, P.O. Box 395, Pretoria 0001, South Africa.
[c]De Beers Consolidated Mines, TSS Technologies, P.O. Box 82851, Southdale, Johannesburg 2135, South Africa.
[d]Department of Chemistry, University of Bath, Claverton Down, Bath BA2 7AY, U.K.
[e]The Royal Institution of Great Britain, 21 Albemarle Street, London W1X 4BS, U.K.
[f]Department of Chemistry, University College London, 20 Gordon Street, London WC1E 6BT, U.K.
*Author for correspondence. E-mail: ngoepep@ul.ac.za

Methods and materials

The bulk crystal structure of pyrite is shown in Fig. 1; it is based on a simple cubic lattice with space group *Pa-3*. The pyrite crystal is best described in terms of the NaCl structure, with the anions replaced by S_2 dimers whose axes are orientated along the four <111> cube directions. Each Fe atom is coordinated to six sulphurs in a slightly distorted octahedron and each sulphur is tetrahedrally coordinated to three Fe atoms and its dimer pair.

Theoretical methods

Common to all computer simulations of condensed matter is the determination of the total energy of the system as a function of the positions of component atoms. Once this energy hypersurface is known, the associated thermodynamic properties can be calculated, including crystal structure, elastic properties, surface energies, and transport properties. The bulk and surface properties of sulphides have been determined by atomistic simulation techniques. These are based on the Born model of solids,[15] which assumes that the ions interact via long-range electrostatic forces and short-range forces which can be determined using simple analytic functions. The components of the short-range forces include both repulsions and the van der Waal's attractions between neighbouring electron charge clouds. The potential model of an atomic assemblage is the set of charges and functional parameters needed to describe all interactions between the component elements. The General Utility Lattice Program (GULP)[16] was used to derive interatomic potentials, and to calculate the bulk properties of pyrite compounds.

Calculations of surface energies of the pyrite compounds were carried out using Metadise code,[17] which is designed to model dislocations, interfaces and surfaces. In this code, the crystal comprises two regions which are periodic in two dimensions. The two blocks together simulate the bulk whereas a single block represents the surface. In the study reported here, region I contains the surface layer and a few atomic layers immediately below it, while region II represents the bulk of the crystal. The ions in region I are allowed to relax to their mechanical equilib-

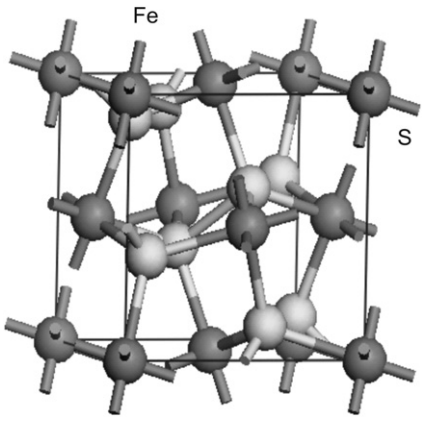

Fig. 1. The FeS_2 pyrite structure, with iron and sulphur represented by darker and lighter shading, respectively.

rium, but those in region II are fixed at their equilibrium positions. Both regions I and II need to be large for the energy to converge.

The surface energy, γ, is evaluated from the energy of the surface block of the crystal $\cup_s$ and the energy of a portion of the bulk crystal U_b, containing the same number of atoms as the surface block. It is given by

$$\gamma = \frac{\cup_s - \cup_b}{A},$$

where A is the surface area. The energies of the blocks are essentially the sum of the energies of interaction of all the component atoms.

In the absence of experimental values, the elastic constants of $PtAs_2$ were determined from electronic structure calculations using planewave pseudopotential methods, as embodied in the CASTEP code,[18] using finite difference methods. The total energy was calculated within the density functional theory framework, and the gradient-corrected approximations GGA–Perdew–Burke–Ernzerhof were used. The wave functions were expanded in a plane-wave basis set with periodic boundary conditions. The interactions between the ionic cores and the electrons were described by ultrasoft pseudopotentials and had a kinetic energy cutoff of 500 eV. In order to use a finite number of wavefunctions, reciprocal space had to be sampled on a discretized set of k-points. We used a special set of 12 k-points as given by the method of Monkhorst and Pack.[19] In optimizations, the total tolerance in the overall energy and pressure change before self-consistency (convergence) was deemed to have been achieved was 2×10^{-5} eV/atom and 0.1 GPa, respectively.

Potential model

The reliability of the calculated structural and elastic properties and surface energies depends on the accuracy of the potential model. Table 1 lists the potential parameters derived and employed in this study for the bulk properties of FeS_2. Those used for surface studies of FeS_2 as pyrite and marcasite are presented in previous work.[13] The potential energy parameters for $PtSb_2$ and $PtAs_2$ are contained in the theses of Mangwejane[20] and Ntoahae,[21] respectively. The short-range interactions between the metal and chalcogenide atoms were fitted to the pyrite structure and optimized using the GULP program. They are described by an effective Buckingham potential:

$$\Phi_{ij}(r_{ij}) = A_{ij}e^{-rij/\rho ij} - C_{ij}/r_{ij}^6,$$

where, classically, the parameter A_{ij} and ρ_{ij} are the size and hardness of the ion, respectively. However, in an effective pair potential, as used here, the A_{ij} and ρ_{ij} terms have become more or less fused. The first term then represents the short-range repulsive interaction between the ions whereas the second term represents the attractive van der Waals' forces.

Table 1. Interatomic potential parameters for FeS_2.

Buckingham potential	A (eV)	ρ (Å)	C (eVÅ^6)
S–S	625.17	0.3308	96.357
Fe–S	29451.7108	0.200259	0.00
Fe–Fe	36224.847	0.3000	0.00
Harmonic	K_{ij} (eVÅ^{-2})	r_0 (Å)	
S–S	6.585968	2.5249	
Three-body	K_{jk} (eV/rad^2)	θ_0	
S–Fe–S	664386.6233	105.485	

The interactions between the sulphur atoms of the S_2 dimer are described by a simple bond harmonic function (called the spring potential):

$$\Phi_{ij}(r_{ij}) = \tfrac{1}{2}k_{ij}(r_{ij} - r_0)^2,$$

where k_{ij} is the bond force constant, r_{ij} the interionic separation and r_0 the separation at equilibrium. k_{ij} and r_0 were obtained from electronic structure calculations of the isolated S_2 dimer.

Finally, a bond-bending term was introduced to allow directionality of bonding between an iron atom and two sulphur atoms which do not belong to the same dimer:

$$\Phi_{ijk}(r_{ijk}) = \tfrac{1}{2}k_{ijk}(\theta_{ijk} - \theta_0)^2,$$

which is a simple harmonic about the equilibrium bond angle, where k_{ijk} is the force constant. $(\theta_{ijk} - \theta_0)$ is the deviation of the bond from the equilibrium angle, which is constrained to the ideal tetrahedral angle of 109.5°. This reflects the fact that sulphur is covalently bonded in a tetrahedral geometry to three iron atoms and to its dimer pair. The elastic constants were found to be fairly sensitive to the force constant and hence allowed us a mechanism for the derivation of k_{ijk}, which was fitted to reproduce the experimental elastic constants.

Results and discussion

Table 2 shows the calculated structural parameters and elastic moduli for pyrite compounds at 300 K; these were compared with experimental measurements and ab initio results where experimental values are not available. The predicted lattice parameter, 5.431 Å, and volume, 160.2 Å^3, for FeS_2 compare well with the experimental values of 5.418 Å and 159.1 Å^3, respectively. The bond lengths and angles are also reproduced to

Table 2. Structural parameters and elastic constants of FeS_2, $PtSb_2$ and $PtAs_2$.

	FeS_2		$PtSb_2$		$PtAs_2$	
	Calc.	Exp.[2]	Calc.	Exp.[11]	Calc.	Exp.[7]
Parameters						
a (Å)	5.431	5.418	6.441	6.440	5.901	5.970
V (Å^3)	160.2	159.1	267.2	267.1	205.5	214.5
Bond length (Å)						
X–X (X–S)	2.179	2.177	2.703	2.670	2.361	2.381
Me–X	2.269	2.262	2.678	2.642	2.468	2.495
Elastic constants (GPa)						
C_{11}	352.6	366.0	265.8	266.0	341.9	355.5$^+$
C_{44}	101.7	105.0	59.17	59.05	97.80	84.93$^+$
C_{12}	47.91	47.00	67.87	68.00	74.10	49.60$^+$
Bulk modulus (GPa)						
B	149.5	155.0	131.9	134.0	163.4	151.6*

$^+$Determined from *ab initio* PWP (planewave pseudopotential method) in the absence of experimental results.
*Determined from *ab initio* PWP using the equation of state.

Table 3. Low-index surface energies of (a) S-terminated pyrite FeS_2; (b) S-terminated marcasite FeS_2; (c) Sb-terminated $PtSb_2$; and (d) As-terminated $PtAs_2$ surfaces.

(**a**)

FeS_2 (pyrite) energy	Unrelaxed surface surface (J/m^2)	Relaxed surface energy (J/m^2)	Termination
{100}	1.30	1.23	S–S–
{110}	2.58	2.36	S–S–
{111}	5.15	3.92	S–S–

(**b**)

FeS_2 (marcasite) surface	Unrelaxed surface energy (J/m^2)	Relaxed surface energy (J/m^2)	Termination
{100}	2.935	2.795	S–S–
{010}	1.292	1.256	S–S–
{101}	1.232	1.232	S–S–
{110}	5.70	4.162	S–S–

(**c**)

$PtSb_2$ surface surface	Unrelaxed surface energy (J/m^2)	Relaxed surface energy (J/m^2)	Termination
{100}	0.948	0.933	Sb–Sb–
{110}	1.679	1.629	Sb–Sb–
{111}	3.054	2.466	Sb–Sb–

(**d**)

$PtAs_2$ surface surface	Unrelaxed surface energy (J/m^2)	Relaxed surface energy (J/m^2)	Termination
{100}	1.10	1.01	As–As–
{110}	1.78	1.62	As–As
{111}	2.93	2.50	As–As–

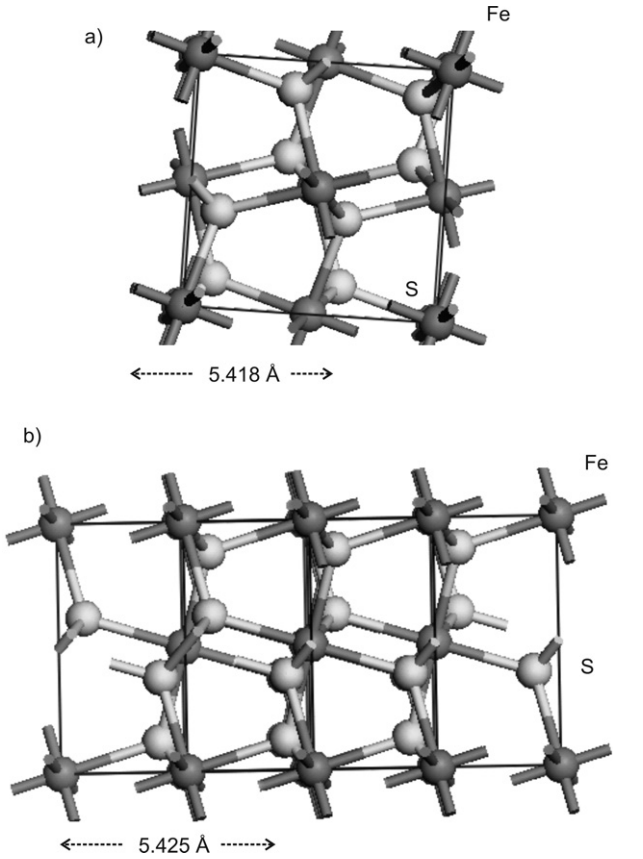

Fig. 2. The arrangement of Fe and S atoms projected on (**a**) a {100} plane for FeS_2 as pyrite; (**b**) on a {101} plane for FeS_2 as marcasite.

within one per cent of measured values. In the case of $PtSb_2$, the calculated lattice parameters and volumes are very close to experimental values and the bond lengths are within 1.2%. As for $PtAs_2$, the calculated lattice parameter differs from experiment by 1.2%, whereas the volume deviates by 3.5%. Overall, we conclude that the derived interatomic potentials yielded reasonably good structural parameters of the pyrite compounds studied.

Elastic constants are normally more difficult to derive from interatomic potentials than structural properties. For FeS_2 the calculated elastic constants C_{11}, C_{44} and C_{12} deviated from experimental values by 3.6%, 3.3% and 1.9%, respectively. The differences in C_{11}, C_{44} and C_{12} for $PtSb_2$ were respectively 0.07%, 0.2% and 0.2%. The calculated elastic constants of $PtAs_2$ are also depicted in Table 2; however, the experimental elastic constants are currently not available. Consequently, the results derived from interatomic potentials were compared with predictions from planewave pseudopotential methods (also calculated in this study); here, the corresponding elastic constants C_{11}, C_{44} and C_{12} differ by 3.8%, 16% and 49.3%, respectively. The calculated bulk moduli for FeS_2 and $PtSb_2$ deviated from experimental values by 3.5% and 1.6%, respectively, whilst that for $PtAs_2$ differed from the planewave pseudopotential bulk modulus by 7.9%. We therefore conclude that, where experimental results are available, the derived pyrite models reproduce elastic constants quite well. In comparing the two sets of calculated elastic constants for $PtAs_2$, it should be noted that *ab initio* results, in certain instances, differed from measured values. Furthermore, for several metal oxides, interatomic potentials were found to be adequate for calculating certain properties, as long as the structure was well reproduced, even though significant differences were observed in most elastic constants. However, we intend to measure the elastic constants of $PtAs_2$, which should lead to further refinements of the interatomic potentials.

Table 3a gives the surface energies of the low-index surface of FeS_2 in pyrite form. The S–S dimers terminate at the surface. The planar {100} surface is the most stable, with the lowest surface energy of 1.23 J/m^2. On energy minimization, the surface relaxes only slightly and remains bulk terminated. *Ab initio* calculated surface energies of pyrite for this configuration are around 1 J/m^2 (ref. 7); Ellmer and Hopfner[23] quote surface energies for the pyrite {100} surface, based on experimental values of the compressibility and bulk moduli, of between 0.54 and 0.82 J/m^2. Our calculated surface energy is within this order of magnitude. Experimental measurements of the surface energy would be valuable for the validation of these results. The other low-index surfaces have higher surface energies and the {111} surface relaxes quite substantially.

The surface energies for the high-index, S–S terminated surfaces of FeS_2 as marcasite are shown in Table 3b. The {101} surface is the most stable and has the same energy as the {100} surface of FeS_2 as pyrite. Indeed, Fig. 2 shows that the arrangement of atoms in the [100] direction of pyrite is similar to that of marcasite in the [101] direction. An electron microscopy study[8] indicated that the intergrowths of marcasite and pyrite are common in which the {101} and {100} surfaces of the respective minerals are parallel. Furthermore, such intergrowths demand that the two structures be virtually identical on the specified planes. Our new potential model predicts the energy equivalence of related surfaces with S termination.

The energies of low-index surfaces of $PtSb_2$ and $PtAs_2$ with the Sb and As terminations are given in Tables 3c and 3d, respectively. As in FeS_2, the {100} surfaces of the two platinum compounds are the most stable, undergo minimal relaxation on

energy minimization and remain bulk terminated. The {110} surface is the next in terms of stability followed by the {111} surface, for which notable relaxations occur. Experimental surface energies for these compounds are currently not available.

Conclusion

We have derived interatomic potentials for some pyrite-structured compounds. Structural properties are well reproduced for FeS_2, $PtSb_2$ and $PtAs_2$ in the bulk, and in the case of FeS_2 the potentials are transferable to the marcasite phase. The elastic constants are generally reasonable, and experimental values are needed for proper validation of $PtAs_2$. Surface energies were calculated for low-index surfaces with the sulphur termination. The {100} surface was predicted to be the most stable for all the pyrite structures in the present study; and underwent minimal relaxation The experimentally observed intergrowth of pyrite and marcasite phases of FeS_2, along the [100] and [101] directions respectively, was supported by the prediction of equal energies of their corresponding surfaces.

We gratefully acknowledge the support of the National Research Foundation and the Royal Society.

1. Vaughan D.J. and Lennie A.R. (1991). The iron sulphide minerals: their chemistry and role in nature. *Sci. Prog. Edinburgh* **75**, 371–388
2. Benbattouche N., Saunders G.A., Lambson E.F. and Holne W. (1989). The dependences of the elastic stiffness moduli and the Poisson ratio of natural iron pyrites (FeS_2) upon pressure and temperature. *J. Phys. D: Appl. Phys.* **22**, 670–675.
3. Schmid-Beurmann P. and Lottermoser T. (1993). ^{57}Fe-Mössbauer spectra, electronic and crystal structures of members of the CuS_2–FeS_2 solid solution series. *Phys. Chem. Minerals* **19**, 571–577.
4. Karguppikar A.M. and Vedeschwar A.G. (1988). Electrical and optical properties of natural pyrite FeS_2 . *Phys. Stat. Sol. (a).* **109**, 549.
5. Sithole H.M., Nyugen-Mahn D., Pettifor D.G. and Ngoepe P.E. (1999). Internal relaxation, band gaps and elastic constant calculations of FeS_2. *Mol. Simul.* **22**, 31–37.
6. Muscat J., Hung A., Russo S. and Yarovsky I. (2002). First principles studies of the structural and electronic properties of pyrite FeS_2. *Phys. Rev. B* **65**, 054107-1–054107-12.
7. Hung A., Muscat J., Yarovsky I. and Russo S.P. (2002). Density-functional theory studies of pyrite FeS_2(100) and (110) surfaces. *Surf. Sci.* **513**, 511–524
8. Dodony I., Mihaly P. and Buseck P.R. (1996). Structural relationship between pyrite and marcasite. *Am. Mineral.* **81**, 119–125.
9. Emtage P.R. (1965). Band structure of platinum antimonide. *Phys. Rev.* **138**, A246–A259.
10. Vaughan D.J. and Craig J.R. (1978). *Mineral Chemistry of Metal Sulfides.* Cambridge University Press, Cambridge
11. Damon D.H., Miller R.C. and Sagar A. (1965). Semiconducting properties of $PtSb_2$. *Phys. Rev.* **138**, A636–A645.
12. Catlow C.R.A. (1997). *Computer Modelling in Inorganic Crystallography.* Academic Press, London.
13. de Leeuw N.H., Sithole H.M., Parker S.C. and Ngoepe P.E. (2000). Modelling surface stability and reactivity of pyrite: introduction of the new potential model. *J. Phys. Chem.* **104**, 7969–7976.
14. Sithole H.M., Ngoepe P.E. and Wright K.W. (2003). Atomistic simulation of the structure and elastic properties of Pyrite (FeS_2) as a function of pressure. *Phys. Chem. Minerals* **30**, 615–619.
15. Born M. and Huang K. (1954). *Dynamical Theory of Crystal Lattices.* Oxford University Press. Oxford
16. Gale J.D. (1997). GULP: a computer program for the symmetry-adapted simulation of solids. *J. Chem. Soc. Faraday Trans.* **93**, 629–637.
17. Watson G.W., Kelsey E.T., de Leeuw N.H., Harris D.J. and Parker S.C. (1996). Atomistic simulation of dislocations, surfaces and interfaces in MgO. *J. Chem. Soc. Faraday Trans.* **92**, 433–438.
18. Segall M.D., Lindan P.L.D., Probert M.J., Pickard C.J., Hasnip P.J., Clark S.J. and Payne M.C. (2002). First-principles simulation: ideas, illustrations and the CASTEP code. *J. Phys.: Cond. Matter* **14**,2717–2743.
19. Monkhorst H.J. and Pack J.D. (1976). Special zones for Brillouin zone integration. *Phys. Rev. B* **13**, 5188–5195
20. Mangwejane S.S. (2005). *Atomistic, electronic and optical studies of $PtSb_2$ and $PtBi_2$.* M.Sc. thesis, University of the North, Sovenga.
21. Ntoahae P.S. (2005). *Applications of computer modelling methods to platinum group minerals.* Ph.D. thesis, University of the North, Sovenga.
22. Ellmer K. and Hopfner C. (1997). On the stoichiometry of semiconductor pyrite (FeS_2). *Phil. Mag. A* **75**, 1129–1151.

Copyright of South African Journal of Science is the property of South African Assn. for the Advancement of Science and its content may not be copied or emailed to multiple sites or posted to a listserv without the copyright holder's express written permission. However, users may print, download, or email articles for individual use.